CrossMark click for updates

Glycolytic flux controls D-serine synthesis through glyceraldehyde-3-phosphate dehydrogenase in astrocytes

Masataka Suzuki[a], Jumpei Sasabe[a,1], Yurika Miyoshi[b], Kanako Kuwasako[c,d], Yutaka Muto[c,d], Kenji Hamase[b], Masaaki Matsuoka[e], Nobuaki Imanishi[a], and Sadakazu Aiso[a]

[a]Department of Anatomy, Keio University School of Medicine, Tokyo 160-8582, Japan; [b]Graduate School of Pharmaceutical Sciences, Kyushu University, Fukuoka 812-8582, Japan; [c]Department of Pharmaceutical Sciences, Faculty of Pharmacy, Musashino University, Tokyo 202-8585, Japan; [d]RIKEN Center for Life Science Technologies, Yokohama 230-0045, Japan; and [e]Department of Pharmacology, Tokyo Medical University, Tokyo 160-8402, Japan

Edited by Solomon H. Snyder, Johns Hopkins University School of Medicine, Baltimore, MD, and approved March 24, 2015 (received for review August 21, 2014)

D-Serine is an essential coagonist with glutamate for stimulation of *N*-methyl-D-aspartate (NMDA) glutamate receptors. Although astrocytic metabolic processes are known to regulate synaptic glutamate levels, mechanisms that control D-serine levels are not well defined. Here we show that D-serine production in astrocytes is modulated by the interaction between the D-serine synthetic enzyme serine racemase (SRR) and a glycolytic enzyme, glyceraldehyde 3-phosphate dehydrogenase (GAPDH). In primary cultured astrocytes, glycolysis activity was negatively correlated with D-serine level. We show that SRR interacts directly with GAPDH, and that activation of glycolysis augments this interaction. Biochemical assays using mutant forms of GAPDH with either reduced activity or reduced affinity to SRR revealed that GAPDH suppresses SRR activity by direct binding to GAPDH and through NADH, a product of GAPDH. NADH allosterically inhibits the activity of SRR by promoting the disassociation of ATP from SRR. Thus, astrocytic production of D-serine is modulated by glycolytic activity via interactions between GAPDH and SRR. We found that SRR is expressed in astrocytes in the subiculum of the human hippocampus, where neurons are known to be particularly vulnerable to loss of energy. Collectively, our findings suggest that astrocytic energy metabolism controls D-serine production, thereby influencing glutamatergic neurotransmission in the hippocampus.

serine racemase | glyceraldehyde-3-phosphate dehydrogenase | D-serine | NADH | glycolysis

Neurons require a great deal of energy owing to their continuous need for ion gradient restoration across the cell membrane. Recent advances in the field of brain energy metabolism strongly suggest that glutamatergic neurotransmission is coupled with molecular signals that switch on glucose utilization pathways to meet this requirement. Astrocytes are key to the energy supply for neurons through the regulation of synaptic glutamate. Astrocytic glutamate uptake drives glycolysis, as well as the subsequent shuttling of lactate from astrocytes to neurons for oxidative metabolism (1–4). Astrocytes also store brain energy currency in the form of glycogen, which can be mobilized to produce lactate for neuronal oxidative phosphorylation (OXPHOS) in response to glutamatergic neurotransmission. Inhibiting glutamate uptake in astrocytes prevents the stimulation of the glycolytic pathway mediated by glutamate (5, 6). In contrast, inhibiting glycolysis impairs glutamate transport or even releases glutamate to the extracellular space (7, 8). These mechanisms suggest that glycolytic metabolism is involved in regulating synaptic glutamate levels and, consequently, in excitatory neurotransmission.

N-methyl-D-aspartate (NMDA) types of glutamate receptors have principal roles in excitatory neurotransmission and participate in numerous physiological processes, including learning and memory. Activity of the NMDA receptor is tightly regulated, and its overactivation contributes to such pathological conditions as stroke (9) and neurodegenerative diseases (10–12). NMDA receptors essentially require binding of a coagonist as well as glutamate for channel opening. D-Serine is a physiological ligand of the coagonist site of NMDA receptors (13). Serine racemase (SRR) converts L-serine into D-serine. SRR and D-serine were first identified in astrocytes, but they also occur in neurons. SRR requires pyridoxal phosphate and also has an absolute requirement for ATP (14, 15). SRR is regulated by interacting proteins, including glutamate receptor interacting protein (GRIP) (16), protein interacting with PRKCA 1 (17), disrupted in schizophrenia 1 (18), and golgin A3 (19). It is also known that the enzymatic activity of SRR is inhibited by nitric oxide in presynaptic neurons (20) and by phosphatidylinositol (4, 5)-bisphosphate (PIP2) in astrocytes (21), both of which are involved in feedback regulation via glutamate receptors. Thus, regulation of D-serine by SRR impacts excitatory neurotransmission through NMDA glutamate receptors. Whether, and if so, how, the glycolytic pathway affects D-serine regulation have remained unknown, however.

In the present study, we show that glycolytic activity directly affects the production of D-serine in astrocytes through interaction between SRR and a glycolytic enzyme, glyceraldehyde 3-phosphate dehydrogenase (GAPDH), and through a glycolytic metabolite, NADH.

Results

Astrocytic D-Serine Is Regulated by Glycolytic Activity. Astrocytes play key roles in modulating both glutamatergic neurotransmission and the energy supply for neurons. We first tested whether

Significance

Neurons require enormous energy to maintain continuous neurotransmission. To meet this requirement, astrocytes support neurons by balancing glycolytic flux with the synaptic level of an excitatory neurotransmitter, glutamate. But to control NMDA-subtype glutamate receptors, regulation of a coagonist, D-serine, as well as of glutamate, is crucial. Here we report that a glycolytic enzyme regulates D-serine synthesis as an indicator of glycolytic activity in astrocytes. This study shows how glutamatergic neurotransmission accommodates to changing energy circumstances through the coagonist.

Author contributions: M.S., J.S., M.M., and S.A. designed research; M.S., J.S., and N.I. performed research; N.I. prepared human tissue samples; M.S., Y. Miyoshi, K.K., Y. Muto, and K.H. contributed new reagents/analytic tools; M.S., J.S., K.K., and Y. Muto analyzed data; and M.S., J.S., and Y. Muto wrote the paper.

The authors declare no conflict of interest.

This article is a PNAS Direct Submission.

[1]To whom correspondence should be addressed. Email: sasabe@a8.keio.jp.

This article contains supporting information online at www.pnas.org/lookup/suppl/doi:10.1073/pnas.1416117112/-/DCSupplemental.

Downloaded at Palestinian Territory, occupied on January 3, 2022

www.manaraa.com

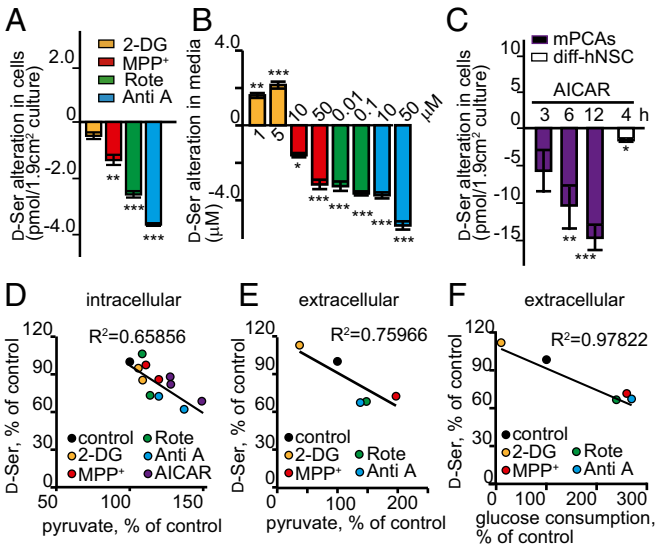

Fig. 1. Glycolysis negatively regulates D-serine. (*A* and *C*) Alterations of intracellular D-serine by 5 mM 2-DG, 100 μM MPP^+, 0.1 μM Rote, 10 μM Anti A, or 1 mM AICAR compared with control (pmol/1.9 cm^2 culture) at 8 h in PCAs (*A*) and at 3, 6, and 12 h in PCAs or diff-hNSCs (*C*) after treatment ($n = 4$ each). (*B*) Alterations of extracellular D-serine concentrations (μM in media) compared with control at 72 h after treatment of the inhibitors at indicated concentrations (μM) ($n = 4$ each). $*P < 0.05$; $**P < 0.01$; $***P < 0.001$, one-way ANOVA followed by Dunnett's multiple-comparison test. Data are plotted as mean ± SEM. (*D–F*) Correlations between D-serine and pyruvate accumulation (*D* and *E*) and glucose consumption (*F*) in cells treated with the indicated inhibitors (*D*) or in the cultured media of cells treated with the indicated inhibitors (*E* and *F*). The *x*-axis represents pyruvate (*D* and *E*) or glucose consumption (*F*) compared with control, and the *y*-axis represents D-serine level compared with control (*D–F*).

activation or inhibition of glycolytic flux affects D-serine production in primary cultured astrocytes (PCAs). Treatment with 1-methyl-4-phenylpyridinium ion (MPP^+), rotenone (Rote), or antimycin A (Anti A), inhibitors of mitochondrial OXPHOS, facilitated glucose consumption at 24–72 h (Fig. S1*A*) and increased intracellular pyruvate at 8 h (Fig. S1*B*) and extracellular pyruvate at 24–72 h (Fig. S1*C*), indicating that inhibition of OXPHOS activated glycolytic flux complementarity (22). This inhibition of OXPHOS reduced both intracellular D-serine (Fig. 1*A*) and extracellular D-serine (Fig. 1*B*). In contrast, 2-deoxyglucose (2-DG), which inactivates glycolysis by inhibiting hexokinase (23, 24), increased extracellular D-serine with reduced extracellular pyruvate and consumption of glucose at 72 h after treatment (Fig. 1*B* and Fig. S1 *A* and *C*), although it affected neither intracellular pyruvate nor D-serine at 8 h (Fig. 1*A* and Fig. S1*B*). None of the inhibitors altered SRR expression in PCAs (Fig. S1 *D* and *E*); rather, the OXPHOS inhibitors accumulated L-serine (Fig. S1*F*), the substrate of SRR, which is positively correlated with extracellular pyruvate level (Fig. S1*G*) but negatively correlated with D-serine (Fig. S1*H*). The enzymatic activity of SRR essentially requires ATP, but the ATP levels did not explain the reduction of D-serine by OXPHOS inhibitors (Fig. S1*I*). Neither a nitric oxide (NO) synthase inhibitor, N^G-nitro-L-arginine methyl ester (L-NAME), nor an NO scavenger, 2-phenyl-4,4,5,5-tetramethylimidazoline-1-oxyl-3-oxide (PTIO), recovered D-serine reduction caused by Anti A, excluding the involvement of SRR inhibition by s-nitrosylation (20) (Fig. S1*J*). Furthermore, no inhibitors triggered more than 20% of cell death even after treatments for 72 h (Fig. S1*K*), showing that alterations in extracellular D-serine cannot be explained by release from dead cells. Antioxidants, such as ascorbate (Asc) and glutathione (GSH), did not recover decreased D-serine by MPP^+ (Fig. S1*L*), suggesting that oxidative stress has no effect on D-serine alteration. That the OXPHOS inhibitors had less influence on extracellular D-serine levels of primary cultured cortical neurons (PCNs) (Fig. S1*M*), which are known to show lower glycolytic activity compared with astrocytes, suggests the correlation between D-serine regulation and glycolytic activity.

We further tested the involvement of glycolysis in modulating D-serine levels using AICA-ribonucleotide (AICAR), an activator of AMP-activated protein kinase (AMPK). AICAR increases AMPK-dependent glucose uptake (25) and facilitates glycolysis through activation of phosphofructokinase (26). As expected, AICAR reduced D-serine with increased pyruvate in mouse PCAs at 6 and 12 h (Fig. 1*C* and Fig. S1*N*) and in differentiated human neural stem cells (diff-hNSCs), including an ∼1:1 ratio of neurons and astrocytes with SRR expression (Fig. S1 *O* and *P*) at 4 h (Fig. 1*C*).

Thus, the negative correlations between intracellular/extracellular D-serine and pyruvate (Fig. 1 *D* and *E*) and between extracellular

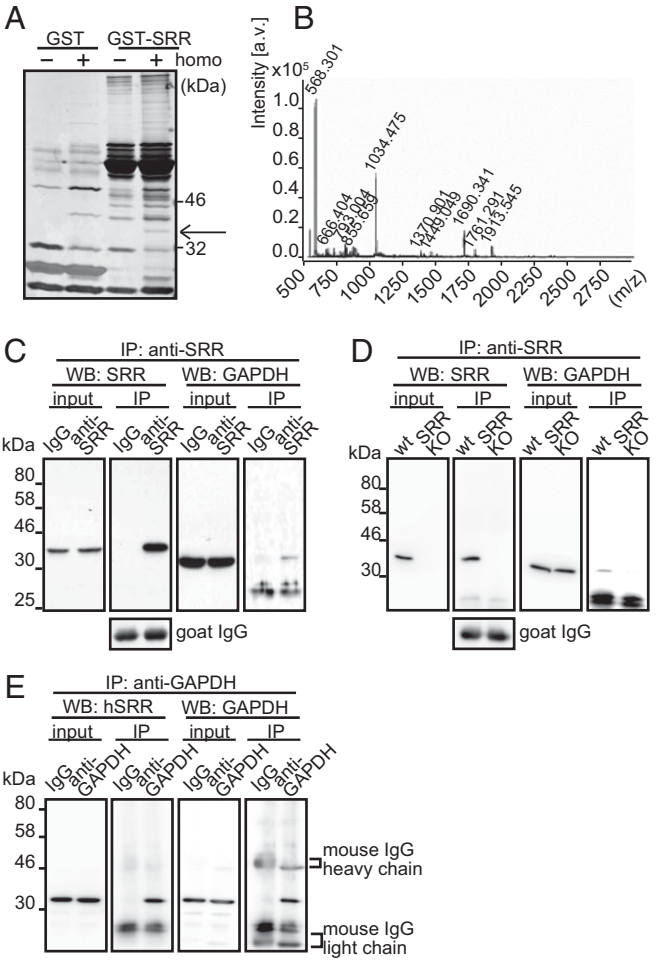

Fig. 2. SRR interacts with GAPDH. (*A*) Pull-down with recombinant GST-SRR was conducted using mouse brain homogenate (homo). The arrow indicates ∼37-kDa protein that specifically interacted with SRR. (*B*) Mass spectra from MALDI-TOF/MS of ∼37-kDa protein. The *y*-axis shows the signal intensity, and the *x*-axis shows the mass-to-charge ratio (*m/z*). (*C*) Endogenous GAPDH was coimmunoprecipitated with a goat anti-SRR antibody from mouse brain homogenate. (*D*) Coimmunoprecipitation of GAPDH with SRR was detected in WT or SRR knockout brain homogenate. (*E*) Endogenous SRR was coimmunoprecipitated with GAPDH in postmortem human brain homogenate and detected on Western blot analysis (WB) with a rabbit polyclonal antibody to human SRR.

Downloaded at Palestinian Territory, occupied on January 3, 2022
www.manaraa.com

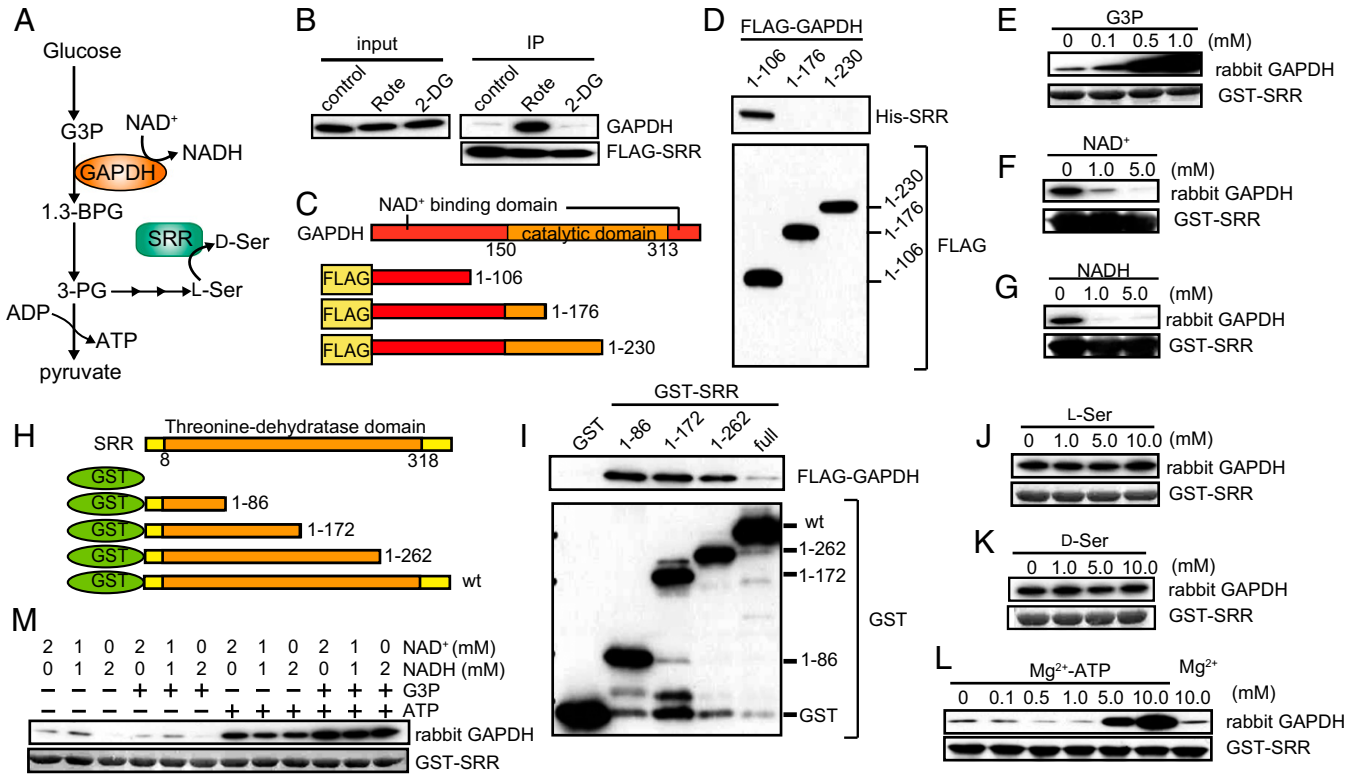

Fig. 3. ATP plays a crucial role in the interaction between SRR and GAPDH. (*A*) Metabolism in glycolysis and the serine biosynthesis pathway. (*B*) Interaction between SRR and GAPDH in A1 cells treated with Rote or 2-DG analyzed by immunoprecipitation with a mouse anti-FLAG antibody, followed by Western blot analysis using a rabbit anti-GAPDH antibody. (*C*) WT and deletion mutants of GAPDH. (*D*) Deletion mutants of FLAG-tagged GAPDH and 6× His-tagged WT SRR were force-expressed in N2a cells. Immunoprecipitation was conducted with the mouse anti-FLAG antibody. SRR interacting with mutant GAPDH was detected by Western blot analysis with a mouse anti-His antibody. (*E*–*G*) Pull-down analysis of rabbit muscle GAPDH with recombinant GST-SRR was conducted in the presence of G3P (*E*), NAD^+ (*F*), or NADH (*G*) at indicated concentrations. (*H*) WT and deletion mutants of GST-SRR. (*I*) Deletion mutants of GST-SRR and FLAG-tagged WT GAPDH were expressed in N2a cells. GST-SRR was pulled down with glutathione beads, and FLAG-GAPDH was detected with the mouse anti-FLAG antibody. (*J*–*L*) Recombinant GST-SRR and purified rabbit muscle GAPDH were pulled down in the presence of L-serine (*J*) and D-serine (*K*), or cofactor Mg^{2+}-ATP (*L*), at the indicated concentrations. (*M*) To mimic intracellular circumstances that are affected by glycolytic activity in vitro, immunoprecipitation was conducted in the presence of NAD^+, NADH, G3P, and/or ATP. Rabbit muscle GAPDH interacting with GST-SRR was detected with the anti-GAPDH antibody.

D-serine and glucose consumption (Fig. 1*F*) indicate that glycolytic flux negatively modulates D-serine level in astrocytes.

GAPDH Interacts with SRR. To search for an SRR-interacting protein related to the glycolytic pathway, we performed a pull-down assay of mouse brain lysate using recombinant SRR fused to GST (GST-SRR). Silver staining showed a protein band of ~37 kDa that interacted specifically with GST-SRR (Fig. 2*A*). MALDI-TOF/MS analysis identified the band as a protein similar to GAPDH, with a Mascot score of 72 (Fig. 2*B*). Endogenous interaction between SRR and GAPDH was confirmed by coimmunoprecipitation of GAPDH in WT or SRR knockout mouse brain lysate with a goat polyclonal anti-mouse SRR antibody (Fig. 2 *C* and *D*), and by coimmunoprecipitation of SRR in human brain lysate with a rabbit polyclonal anti-human GAPDH antibody (Fig. 2*E*).

Immunocytochemical analyses with a monoclonal anti-SRR antibody, which can label mouse SRR in the cells (Fig. S2*A*), showed exogenously expressed SRR colocalized with endogenous GAPDH mostly in soma and partly around the perinuclear region or plasma membrane in PCAs (Fig. S2 *B*–*D*). There was an increasing tendency, albeit without statistical significance, to colocalize when PCAs were treated with Anti A (Fig. S2*E*). On the other hand, in PCNs, exogenously expressed SRR was localized to soma and neural processes, colocalizing with GAPDH mostly in soma (Fig. S2 *F*–*H*). Rote treatment on neurons decreased colocalization of SRR and GAPDH (Fig. S2*I*), indicating that SRR is differently regulated in astrocytes and in neurons.

Glycolysis Regulates the Interaction Between SRR and GAPDH Through ATP. GAPDH not only catalyses the sixth step of glycolysis (Fig. 3*A*), but also has been implicated in multiple nonmetabolic processes. Therefore, we assumed that glycolysis affects the interaction between SRR and GAPDH. In fact, immunoprecipitation of GAPDH with FLAG-SRR in the presence of Rote or 2-DG showed that activating glycolysis augmented the interaction between SRR and GAPDH, whereas inhibiting it did not change the interaction in A1 astrocytoma cells (Fig. 3*B*). We further confirmed, using PCAs, that the endogenous interaction between SRR and GAPDH was augmented by MPP^+, Rote, Anti A, or AICAR (Fig. S3 *A*–*D*), indicating that activating glycolysis facilitates the interaction between SRR and GAPDH.

We next examined how glycolysis affects the interaction between GAPDH and SRR. GAPDH is composed of two folding domains, an NAD^+-binding domain (residues 2–150) and a catalytic domain (residues 155–312). We constructed three deletion mutants of GAPDH that lack different lengths in their C-terminal regions ($GAPDH^{1–106}$, $GAPDH^{1–176}$, and $GAPDH^{1–230}$) (Fig. 3*C*). Among these three mutants, $GAPDH^{1–106}$ showed an affinity with SRR, whereas $GAPDH^{1–176}$ and $GAPDH^{1–230}$ did not (Fig. 3*D*), suggesting that the catalytic domain interrupts interacting sites in the NAD^+-binding domain of GAPDH. Therefore, we speculated that GAPDH would require a conformational change to interact with SRR. Indeed, in vitro binding assays with substrates of GAPDH revealed that glyceraldehyde-3-phosphate (G3P) augmented the SRR–GAPDH interaction in a dose-dependent

Downloaded at Palestinian Territory, occupied on January 3, 2022
www.manaraa.com

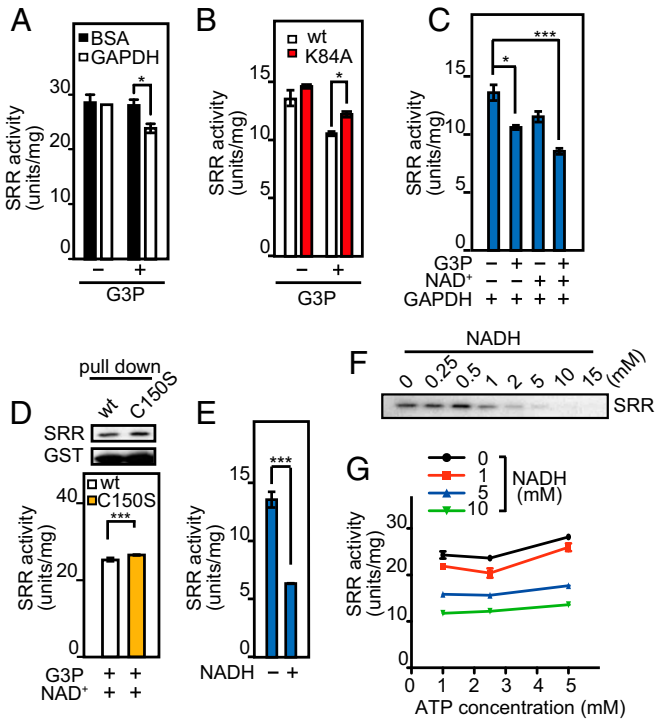

Fig. 4. GAPDH inhibits SRR activity through direct interaction and NADH production. (*A*) D-Serine production by recombinant SRR in the presence of BSA or GAPDH with G3P was analyzed with 2D-HPLC ($n = 3$ each). $^{*}P < 0.05$, Student *t* test. (*B*) Synthesis of D-serine by recombinant SRR in the presence of WT or K84A GAPDH with or without G3P was measured ($n = 4$ each). $^{*}P < 0.05$, Student *t* test. (*C*) SRR activities were measured in the presence of G3P, NAD^+, or both ($n = 4$ each). $^{*}P < 0.05$, $^{***}P < 0.001$, one-way ANOVA followed by Dunnett's multiple-comparison test. (*D*) SRR was pulled down with GST-fused WT or C150S-GAPDH (Upper, Western blots with antibodies to SRR and GST). D-Serine synthesis by SRR with WT or C150S-GAPDH in the presence of G3P and NAD^+ was quantified using 2D-HPLC (n = 4 each). $^{*}P < 0.05$, Student *t* test. (*E*) SRR activity was analyzed with or without NADH (n = 4 each). $^{***}P < 0.001$, Student *t* test. (*F*) Recombinant SRR was pulled down with ATP-agarose beads in the presence of NADH and detected by the anti-SRR antibody in Western blot analysis. (*G*) D-Serine production by recombinant SRR was measured in vitro using 2D-HPLC in the presence of NADH and ATP at various combinations of doses. The reaction time with SRR in each experiment was 3 h (*A*, *B*, *C*, and *E*) or 15 h (*D*). Data are plotted as mean ± SEM.

manner (Fig. 3*E*), whereas NAD^+ and its reduced form, NADH, inhibited the interaction (Fig. 3 *F* and *G*). Alanine-scanning mutagenesis of residues on the surface of the NAD^+-binding domain of GAPDH revealed that several mutants significantly attenuated the binding to SRR (Fig. S4*A*). These results indicate that glycolytic metabolites control the GAPDH binding to SRR with a broad interface consisting of several hydrophobic sites in the NAD^+-binding domain (Fig. S4*B*).

To study the interacting site in SRR, we created C-terminal truncated mutants $SRR^{1–86}$, $SRR^{1–172}$, and $SRR^{1–262}$ (Fig. 3*H*). Each truncation of the C-terminal regions of SRR significantly augmented the interaction with FLAG-tagged GAPDH in vitro (Fig. 3*I*), suggesting that the C-terminal residues 263 to 339 in SRR inhibit the binding of GAPDH. The substrates of SRR, L-serine and D-serine, did not affect the interaction (Fig. 3 *J* and *K*); in contrast, Mg^{2+}-ATP, a physiological activator of SRR (14), augmented the interaction in a dose-dependent manner (Fig. 3*L*).

To identify the metabolite responsible for regulating the interaction between SRR and GAPDH in glycolysis, we performed a pull-down assay of GAPDH with GST-SRR in the mixture of NAD^+, NADH, G3P, and/or ATP in vitro. In the absence of ATP, NADH inhibited the interaction, which was not recovered by addition of G3P. In contrast, in the presence of ATP, the inhibitory effects of NAD^+ and NADH were nullified, and G3P strengthened the interaction (Fig. 3*M*). Given that glycolytic activation by OXPHOS inhibitors sustained high intracellular ATP levels in astrocytes, these results suggest that ATP mainly augments the interaction between SRR and GAPDH in glycolytic activation.

GAPDH Inhibits SRR Activity Through Direct Interaction and Production of NADH. To investigate the functional roles of GAPDH in SRR activity, we measured D-serine produced by recombinant SRR in the presence of GAPDH with G3P and ATP in vitro. GAPDH inhibited D-serine production when incubated with G3P (Fig. 4*A*). Inhibition of SRR activity by GAPDH was partly restored by substitution of Lys84 in GAPDH with Ala (K84A) (Fig. 4*B*), which strikingly reduced the interaction with SRR without affecting the enzymatic activity of GAPDH (Figs. S4*A* and S5*A*), suggesting that GAPDH directly inhibited SRR activity through binding, at least in part.

In glycolysis, GAPDH catalyzes the NAD^+-dependent oxidation of G3P into 1,3-bisphosphoglycerate and NADH. We speculated that metabolites in the enzymatic reaction of GAPDH also affect SRR activity, because the reduction of D-serine production by G3P was further enhanced by addition of NAD^+ in the presence of GAPDH (Fig. 4*C*). A C150S mutant of GAPDH, with decreased GAPDH activity to one-half that of WT (Fig. S5*A*), mildly but significantly recovered the inhibitory effect of GAPDH in the presence of G3P and NAD^+ without affecting the interaction between GAPDH and SRR (Fig. 4*D*). Indeed, we found that NADH solely inhibited SRR activity in vitro (Fig. 4*E*), indicating that metabolites of GAPDH also inhibit SRR activity. Both ATP and NADH include ADP ribose in their framework (Fig. S5*B*), and NADH detached binding of ATP to SRR in a dose-dependent fashion (Fig. 4*F*); however, ATP did not compete with the inhibitory effect of NADH (Fig. 4*G*), suggesting that NADH allosterically inhibits SRR activity by destabilizing SRR. In support of this view, analysis by circular dichroism (CD) of recombinant SRR indicated that the alpha-helix structure in the presence of ATP, estimated with an abyss of spectrum at 208 nm, was distorted by the addition of NADH (Fig. S5 *C* and *D*). The inhibitory effect of NADH tested in PCAs was reduced in the oxidized form, NAD^+, and was nullified in the removed form of ADP ribose, nicotinamide (NAM) (Fig. S5*E*). Together with our finding that MPP^+ or Anti A increased intracellular NADH in astrocytes (Fig. S5 *F* and *G*), these results indicated that activation of glycolysis inhibited D-serine production through the dual effects of GAPDH on SRR: direct interaction and destabilization by NADH.

Astrocytes Express SRR in the Subiculum of Human Hippocampal Formation. In rodents, the astrocytic expression of SRR is controversial. Although astrocytes express SRR at higher levels than neurons in vitro (Fig. S6*A*), SRR expression in vivo is found predominantly in neurons (27). On the other hand, astrocyte-specific knockout of SRR reduced its protein level by 15% (28), and mice expressed with eGFP under the mouse *SRR* promoter have shown eGFP expression not only in neurons, but also in astrocytes in hippocampus (29). To clarify the expression of SRR in mouse astrocytes in vivo, we enriched SRR-positive immunohistochemical signals by enhancing the reaction between antigen and primary antibody and amplifying the fluorescent labeling onto secondary antibody. The SRR-positive signals were detected not only in neurons, but also (albeit mildly) in astrocytes in hippocampus of WT mice, but not of SRR knockout mice (Fig. S6 *B* and *C*).

To search further for SRR-positive astrocytes in human hippocampus, which are known to be vulnerable to various insults including hypoglycemia, we performed an immunohistochemistry analysis of postmortem human hippocampal formation. The specificity of an anti-human SRR (hSRR) antibody was validated in Western blot and immunohistochemistry analyses (Fig. S6 *D*–*H*).

Downloaded at Palestinian Territory, occupied on January 3, 2022
www.manaraa.com

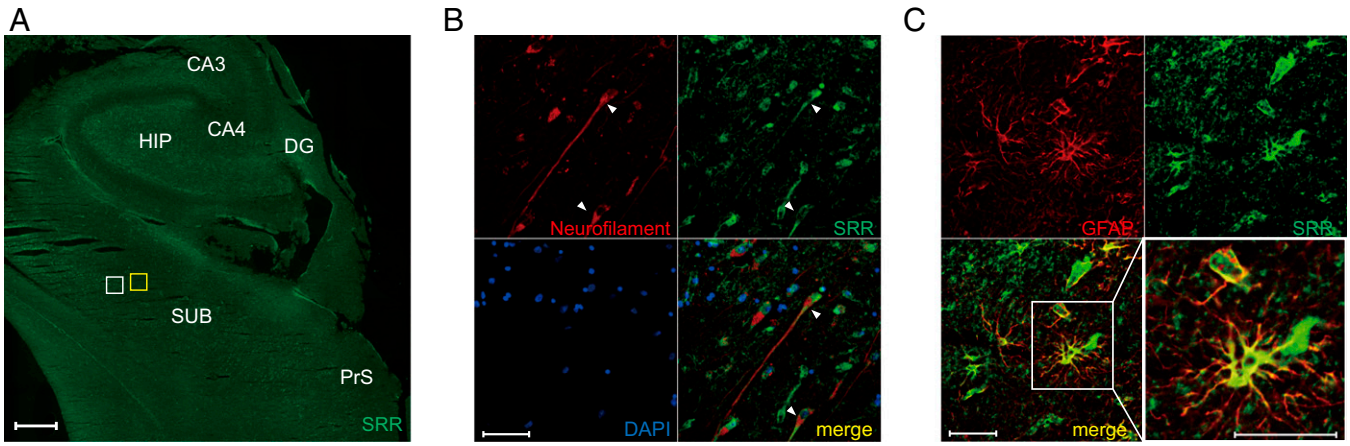

Fig. 5. Astrocytes express SRR in the human subiculum. (*A*) Tissue section of hippocampal formation was immunolabeled with anti-human SRR antibody. (Scale bar: 1 mm.) DG, dentate gyrus; HIP, hippocampus; PrS, presubiculum; SUB, subiculum. (*B* and *C*) Enlarged view of the yellow (*B*) and white (*C*) squares in *A*. Sections were stained with antibodies to neurofilament L (*B*; red) or GFAP (*C*; red) and human SRR (green). Arrowheads show pyramidal neurons. In *C*, *Lower Right* is a high-magnification view of *Lower Left*. (Scale bars: 50 μm.)

SRR was widely observed in neurons in the subiculum (white frame in Fig. 5*A*, enlarged in Fig. 5*B*) and the multiform layer (Mul), but not in the molecular layer (Mol) of the dentate gyrus (Fig. S6*I*). In contrast, astrocytic SRR was observed in the subiculum (yellow frame in Fig. 5*A*, enlarged in Fig. 5*C*), but not in the dentate gyrus (Fig. S6*J*). Because the subiculum relays fibers from CA1 pyramidal neurons and entorhinal cortical neurons to the prefrontal cortex, mammillary nucleus, amygdala, and hypothalamus, glycolytic regulation of astrocytic D-serine may play a role in the glucose-sensitive hippocampal neural circuits.

Discussion

Our results suggest a new aspect of the cross-talk between glycolysis and glutamatergic neurotransmission. We have shown that glycolytic flux controls the synthesis of D-serine, a physiological coagonist with glutamate at NMDA-subtype glutamate receptors, through a glycolytic enzyme and metabolite in astrocytes (Fig. 6). ATP synthesis driven by glycolysis enhances the interaction between GAPDH and SRR, which in turn inactivates D-serine synthesis by SRR. Using mutants of GAPDH, we have demonstrated that both the binding of GAPDH and of NADH produced by GAPDH will inhibit SRR activity in a coordinated manner.

The biosynthesis pathway of D-serine starts from a glycolytic intermediate, 3-phosphoglycerate, in the central nervous system. After three-step reactions from the intermediate, L-serine is synthesized in astrocytes and then converted into D-serine by SRR (30). Both serine enantiomers are deeply related to neurophysiology; L-serine is a neurotrophic factor essential for brain morphogenesis (31, 32), whereas D-serine is a prerequisite for glutamatergic neurotransmission mediated by synaptic NMDA receptors (13, 18, 33–35). Considering that L-serine is also known to control glycolytic flux through the M2 isoform of pyruvate kinase (36), neurophysiology through serine biosynthesis is inseparable from glycolysis. In the present study, we found that glycolytic flux regulates D-serine synthesis by SRR independent of the serine biosynthesis pathway (Figs. 1 and 6), which suggests that glycolysis can affect glutamatergic neurotransmission with no interference in the neurotrophic effect of L-serine. This direct impact of glycolytic flux on D-serine synthesis may be important for neurons, which require a continuous energy supply for neurotransmission, to promptly accommodate to altered energy circumstances. Because inhibiting glycolysis reduces glutamate uptake and releases glutamate and D-serine from astrocytes (7, 8) (Fig. 1), regulation of D-serine synthesis by glycolysis is assumed to modulate excitatory neurotransmission in concert with glutamate.

For full activity, SRR requires binding of a cofactor, PLP (37), as well as Mg^{2+}-ATP (14, 15). ATP is not hydrolyzed by SRR, and both ATP- and Mg^{2+}-binding sites are located outside a catalytic site (38); therefore, Mg^{2+}-ATP is thought to stabilize the folding of SRR (39). Our finding that Mg^{2+}-ATP augments the interaction between SRR and GAPDH implies the need for SRR folding for the interaction. In accordance with a report that SRR activity reached a plateau at >1 mM ATP (15), ATP augmented the interaction between GAPDH and SRR at >1 mM (Fig. 3*L*), supporting our idea that GAPDH inactivates stabilized SRR with ATP binding.

We have also shown that NAD^+ and NADH inhibit SRR activity (Fig. 4 and Fig. S5). Despite the structural resemblance of NADH and ATP (Fig. S5*B*), the inhibitory effect of NADH cannot be competed by ATP (Fig. 4*G*). Given that ATP stabilizes folding of SRR, detachment of ATP from SRR in the presence of NADH (Fig. 4*F*) indicates that NADH destabilizes the alpha-helix structure (Fig. S5 *C* and *D*) and allosterically inhibits the activity of SRR. Together with the fact that physiological intracellular ATP and NADs are found at levels of several millimolars in astrocytes (40–43), NADs seem to regulate SRR activity more sensitively than ATP. Furthermore, considering that NADH is a more potent inhibitor than NAD^+ (Fig. S5*E*), the intracellular NADH/NAD^+ ratio may be negatively correlated with SRR activity. Thus, our data suggest that GAPDH inhibits SRR activity in two steps: (*i*) capturing ATP-bound SRR and (*ii*) destabilizing SRR by NADH.

Another aspect of our study concerns the expression of SRR in astrocytes. SRR was first identified as a glial enzyme (44), but more recent studies using SRR knockout mice have shown that SRR is expressed primarily in neurons found in the cerebral cortex and hippocampus (27, 45). On the other hand, the possibility of SRR expression in astrocytes cannot be excluded, given the following evidence: (*i*) astrocyte-specific knockout of SRR reduces its expression level by 15% in the brain (28); (*ii*) eGFP designed to express under the SRR promoter in mice is detectable in hippocampal astrocytes (29); and (*iii*) enhancement of immunohistochemical signal makes astrocytic SRR observable (Fig. S6*B*). Given the high glycolytic activity in astrocytes, the use of primary cultured astrocytes in our experimental model explaining the effect of glycolysis on SRR to primary cultured astrocytes is appropriate. In fact, the effect of OXPHOS inhibitors was less prominent in primary cultured neurons than in astrocytes (Fig. S1*R*); however, we do not exclude the possibility that GAPDH also may be inhibiting SRR activity in neurons, considering that both GAPDH and SRR are expressed abundantly in neurons in

Downloaded at Palestinian Territory, occupied on January 3, 2022
www.manaraa.com

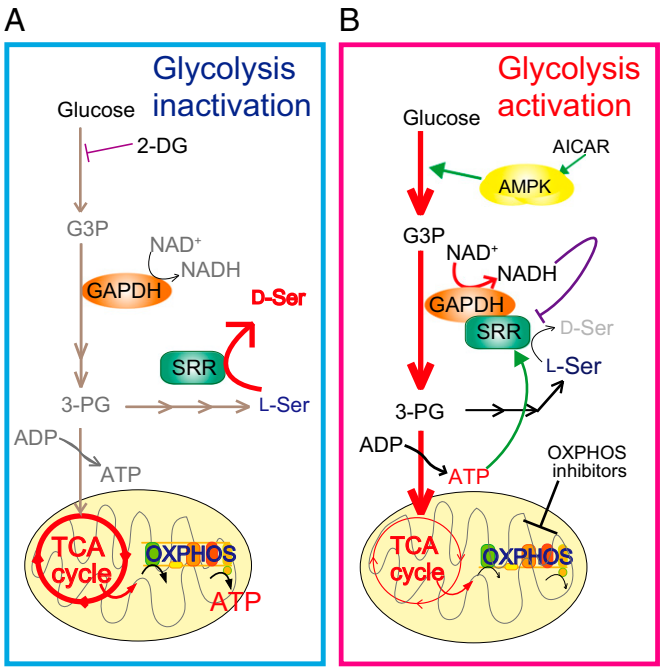

Fig. 6. Schematic illustration of D-serine regulation through glycolysis. (*A*) Inhibition of hexokinase by 2-DG decreases glyoclytic flux, leading to impaired interaction between SRR and GAPDH. Free SRR facilitates D-serine production. (*B*) Inhibition of OXPHOS or activation of AMPK activates glycolysis in astrocytes, which increases levels of ATP and NADH. ATP augments the interaction between SRR and GAPDH. The interaction with GAPDH inhibits D-serine synthesis by SRR by (*i*) direct inhibition of SRR activity through binding of GAPDH and (*ii*) exposure of SRR to NADH metabolized by GAPDH.

mouse and human brains. In accordance with previous reports, immunohistochemistry of SRR showed a predominant distribution in neurons in human hippocampal formation, but with astrocytic SRR seen in the subiculum as well (Fig. 5).

The subiculum is a pivotal structure positioned as an interface between the hippocampus proper and the entorhinal and other cortices, as well as in a range of subcortical structures. Given their crucial neuroanatomic position, and considering that hippocampal formation including the subiculum is vulnerable to energy depletion, subicular astrocytes may play important roles in controlling energy supply and neurotransmission. Although the functional properties of the subiculum are not well understood, its impairment results in the loss of spatial navigation, mnemonic processing, and control of the response to stress (46), suggesting that regulating D-serine in subicular astrocytes in response to various energy circumstances could affect memory and emotion.

Our findings reinforce the importance of glycolytic flux in the regulation of glutamatergic neurotransmission through direct inactivation of the enzyme producing the coagonist of NMDA glutamate receptors.

Materials and Methods

Animals. Crlj:CD-1 (ICR) mice were purchased from Charles River Laboratories Japan. SRR knockout mice were kindly provided by Dr Ryuichi Konno (47). All animal experiments were approved by Keio University's Institutional Animal Experiment Committee.

Human Samples. Human hippocampal tissue was collected from a cadaver donated after death with prior consent at Keio University School of Medicine. The cadaver, an 88-y-old Japanese woman who had died of cholangiocellular cancer, was examined at 40 h postmortem. Neuropathological assessment of the brain did not identify any metastasis of cancer or neurodegenerative abnormalities other than minor age-related changes. The body was perfused with ice-cold PBS (pH 7.4) from the thoracic aorta, after which the specimens were dissected and processed for histological analysis.

Materials. Mg^{2+}-ATP, NAM, NAD^+, NADH, G3P, rabbit muscle GAPDH, 2-DG, MPP^+ iodide, Rote, Anti A, AICAR, and glutathione were purchased from Sigma-Aldrich. PTIO and L-NAME were purchased from Tokyo Chemical Industry. Ascorbate was purchased from Wako Pure Chemical Industries. Neurobasal medium, B27 supplement, DMEM with high glucose, Opti-MEM, Lipofectamine 2000, GlutaMAX, and penicillin-streptomycin solution were purchased from Life Technologies.

Antibodies. A rabbit polyclonal antibody to hSRR was purchased from Abcam. A mouse monoclonal antibody to FLAG tag and its HRP-conjugated form, and a rabbit anti-actin polyclonal antibody, were purchased from Sigma-Aldrich. A mouse monoclonal antibody to glial fibrillary acidic protein (GFAP), Neurofilament-L, and a rabbit monoclonal antibody to GAPDH (14C10) were obtained from Cell Signaling Technology. A mouse monoclonal antibody to NeuN was obtained from Millipore. A goat polyclonal antibody to mouse SRR and mouse monoclonal antibodies to GAPDH (6C5), to 6× His, and to GST were obtained from Santa Cruz Biotechnology. FITC-conjugated anti-mouse IgG, Texas red-conjugated anti-mouse IgG, and Texas-red conjugated anti-rabbit IgG were purchased from Jackson ImmunoResearch Laboratories. Mouse monoclonal antibody to SRR was purchased from BD Biosciences.

Cell Culture and Transfection. PCAs were prepared from freshly dissected cortices of mouse embryos at embryonic day 14 and disassembled with papain, then cultured in Neurobasal medium containing 2% (vol/vol) B27 supplement, 1% GlutaMax and 1% penicillin-streptomycin. At 1 d in vitro (DIV), cultured media were replaced with DMEM containing 10% (vol/vol) FBS and 1% penicillin-streptomycin. Cultured media were replaced with fresh media every 3 d thereafter. At 14 DIV, the cultured cells were differentiated into astrocytes.

Mouse A1 astrocytoma cells and neuronal N2a cells were cultured in DMEM containing 10% FBS and 1% penicillin-streptomycin.

Full-length FLAG-SRR, His-SRR, GST-SRR, deletion mutants of GST-SRR, and deletion mutants of FLAG-GAPDH were expressed with Lipofectamine 2000 following the manufacturer's protocol.

Measurement of D-Serine. D-Serine in in vitro SRR activity assays, in cells, or in cell-cultured media was quantified by HPLC as described previously (48–50). In brief, samples were mixed with methanol and centrifuged to remove protein depositions. To determine intracellular D-serine, PCAs were washed twice in PBS and suspended in 20 μL of lysis buffer (50 mM Tris·HCl, 15 mM NaCl, 20 mM EDTA, and 1% Triton X-100, pH 7.4). After addition of 80 μL of methanol and centrifugation at 20,400 × *g* for 10 min, supernatants were spin-dried and resuspended in 20 μL of 200 mM sodium borate (pH 8.0). Then the resuspension was mixed with 5 μL of 40 mM NBD-F in acetonitrile (ACN) and then incubated at 60 °C for 2 min. The reaction was stopped by the addition of 75 μL of 2% (vol/vol) TFA. NBD derivatives were injected into a 2D-HPLC system (NANOSPACE SI-2 series; Shiseido). Total serine was separated by a monolithic ODS column (750 mm × 0.53 mm I.D., prepared in a fused silica capillary provided by Shiseido). The enantiomers were further separated by a Sumichiral OA-2500S column using (S)-naphthylglycine as a chiral selector (250 mm × 1.5 mm I.D. self-packed material; Sumika Chemical Analysis Service). The NBD-serine enantiomers were detected at 530 nm with excitation at 470 nm.

Plasmid Construction. Total RNA of mouse cerebral cortex and human cerebral cortex was extracted with RNAiso extraction reagent (Takara), and cDNA was produced using a Primescript RT-PCR Kit (Takara). Mouse *SRR* (mSRR) and *GAPDH* were cloned from mouse cDNA, and human *SRR* (hSRR) was from human cDNA. Then these cDNAs were subcloned into pGEX 5X-1 or pCAG-GSKS vector using an In-fusion Advantage PCR Cloning Kit (Clontech). GST-tagged mSRR was subcloned from pGEX 5X-1 into pEF1 vector. FLAG tag was added to the N-terminal ends of GAPDH and mSRR using the KOD Plus Mutagenesis Kit (Toyobo). Deletion mutants of pEF1 GST-mSRR and pCAG FLAG-GAPDH were constructed with the KOD Plus Mutagenesis Kit with primers designed to be near the deletion loci, following the manufacturer's protocol.

Purification of Recombinant Protein. Competent high-DH5α cells (Toyobo) were transformed with pGEX2T or pGEX5X-1 mSRR plasmid, grown in LB medium with ampicillin at 37 °C overnight. Expression of GST-SRR was induced by incubation with 0.1 mM isopropyl-1-thio-β-D-galactopyranoside at 28 °C for 6 h. Bacteria were lysed and sonicated in 0.2% Triton X-100 PBS. GST-SRR recombinant protein was then precipitated with Glutathione

Downloaded at Palestinian Territory, occupied on January 3, 2022
www.manaraa.com

Sepharose 4B beads (GE Healthcare) at 4 °C for 2 h. After five washes in PBS, the recombinant protein was stored at 4 °C until use. For the SRR activity assay, GST-SRR was dissociated in a reaction buffer (0.08 U/mL Factor Xa, 50 mM Tris·HCl pH 7.5, 150 mM NaCl, 1 mM $CaCl_2$) with constant rotation at room temperature for longer than 10 h. The eluent was mixed with slurry of Xarrest agarose (EMD Millipore) at room temperature for 10 min and dialyzed with a dialytic membrane (molecular weight cutoff 14,000; Viskase) in PBS at 4 °C overnight.

Pull-Down Assay. Mouse whole brain was dissected and homogenized in a lysis buffer (50 mM Tris·HCl pH 7.4, 15 mM NaCl, 20 mM EDTA, 1% Triton X-100, and protease inhibitor mixture) and centrifuged at 20,400 × *g* for ∼10 min until the supernatant became clear. The supernatant was mixed with glutathione Sepharose beads fused with recombinant GST-SRR in an immunoprecipitation (IP) buffer (20 mM Hepes-NaOH pH 7.4, 1 mM DTT, 1 mM EDTA, 150 mM NaCl, and 0.1% Triton X-100) at 4 °C for 2 h. Then the beads were washed several times in the IP buffer. After being denatured in a sample buffer [100 mM Tris·HCl, 5% (wt/vol) SDS, 25% (vol/vol) glycerol, and 0.05% bromophenol blue] at 95 °C for 5 min, the protein was stored at 4 °C until the next procedure.

Silver Staining. Samples obtained by pull-down assay were subjected to SDS/PAGE. After electrophoresis, the polyacrylamide gel was fixed in 10% (vol/vol) MeOH, 7.5% (vol/vol) acetate, and 0.05% HCHO for 45 min and then washed in Milli-Q water for 35 min, reduced in 0.5% DTT for 40 min, stained with 0.1% $AgNO_3$ for 1 h, washed in Milli-Q water for 1 min, and developed with 0.05% HCHO and 3% (wt/vol) Na_2CO_3. The staining was terminated by the addition of 5% acetic acid.

MALDI-TOF/MS. Protein interacting with GST-SRR was pulled down from mouse brain lysate as described above. A protein band visualized with Coomassie brilliant blue staining was excised and decolorized in 50 mM $(NH_4)HCO_3$ and 50% ACN. The piece of gel was dehydrated with ACN and dried in a vacuum centrifuge. Then the protein in the gel was digested into peptides in 99 mM $(NH_4)HCO_3$, 0.01% trypsin, and 0.2% n-octyl glucoside at 37 °C overnight. The digested peptides were extracted in 0.05% trifluoroacetate (TFA) and 50% (vol/vol) ACN and dried in a vacuum centrifuge. The peptides were resuspended in 0.1% TFA and purified with Zip Tip (Millipore). Finally, peptides were dissolved in 0.05% TFA and 50% ACN. Peptide sequences were analyzed by MALDI-TOF/MS (Autoflex III; Bruker Daltonics), using MASCOT Search with a NCBInr database.

Immunoprecipitation. Mouse or human brain lysate was precleared with protein G Sepharose beads (GE Healthcare) in the IP buffer. The goat polyclonal antibody to mSRR was incubated with protein G Sepharose beads at 4 °C for 2 h, mixed with the precleared brain lysate, and incubated under constant rotation at 4 °C. The beads were then washed four times in the IP buffer and subjected to SDS/PAGE. GAPDH and SRR precipitated with the beads were detected by Western blot analysis with the anti-GAPDH rabbit monoclonal antibody (14C10; 1:1,000) or anti-SRR mouse monoclonal antibody (1:1,000). For coimmunoprecipitation of human SRR with human GAPDH, a mouse polyclonal antibody to GAPDH was conjugated with protein G Sepharose beads and mixed with human brain lysate. After washing with IP buffer, the sample was subjected to Western blot analysis. SRR precipitated with GAPDH was detected by Western blot analysis with the rabbit polyclonal anti-human SRR antibody (1:1,000) or mouse monoclonal anti-GAPDH antibody 6C5 (1:1,000).

In Vitro Binding Assay. Recombinant GST-SRR was purified with glutathione beads and mixed with rabbit muscle GAPDH in the IP buffer with NAD^+, NADH, G3P, L-serine, D-serine, and/or ATP. After constant rotation at 4 °C for 1 or 2 h, the beads were washed five times in the IP buffer. The samples were then subjected to SDS/PAGE, and GAPDH was detected by Western blot analysis with an anti-GAPDH mouse monoclonal antibody.

SRR Activity Assay. Recombinant SRR detached from GST and purified as described above was mixed with recombinant WT, K84A, or C150S mutant GAPDH in an SRR reaction buffer (50 mM Tris·HCl pH 8.2, 10 μM PLP, and 1 mM $MgCl_2$). Then L-serine at a final concentration of 5 mM was added to start the assay. After incubating the mixture at 37 °C, production of D-serine was determined by HPLC. SRR activity (unit/mg) was calculated by amount (μmol) of D-serine produced by SRR, SRR protein (mg), and reaction time (h).

ATP-Binding Assay. Purified recombinant SRR was mixed with ATP agarose (Sigma-Aldrich) in IP buffer with NADH at the indicated concentrations, then washed several times with the IP buffer and subjected to SDS/PAGE. Western blot analysis was performed with the mouse monoclonal anti-SRR antibody.

Immunohistochemistry. Postmortem human hippocampus was fixed in 4% paraformaldehyde (PFA) PBS for 18 h and dehydrated in 20% (wt/vol) sucrose PBS. The tissue block was placed in an embedding mixture (OCT compound: 20% sucrose in PBS, 5:2) and sliced to a thickness of 10 μm. The slices were then attached to MAS-coated glass slides (Matsunami Glass). Tissue sections were washed twice in PBS, treated with methanol containing 0.3% H_2O_2 for 10 min, and blocked in a blocking reagent (Dako) for 2 h and in 5% (vol/vol) goat serum PBS overnight. The sections were immunolabeled for 3 d with rabbit anti-human SRR antibody (1:100) and mouse anti-GFAP (1:100) antibody in PBS containing 5% goat serum at 4 °C. After three washes in PBS, the sections were incubated with goat anti-rabbit IgG biotinylated antibody and Texas red-conjugated anti-mouse IgG in 5% goat serum PBS for 1 h. The biotinylated antibody was visualized with a Tyramid Signal Amplification system (PerkinElmer) in accordance with the manufacturer's protocol. After three washes with PBS, sections were covered with a Prolong Gold Antifade Reagent with DAPI (Life Technologies).

Statistical Analysis. All values in the text and figures are reported as mean ± SEM. Statistical analyses for the experiments were performed with the two-tailed Student *t* test or one-way ANOVA followed by Dunnett's multiple-comparison test, in which $P < 0.05$ was assessed as significant. All analyses were performed using Prism 5 (GraphPad Software). Linear correlation was analyzed by Pearson product-moment correlation coefficient with Microsoft Excel software. Coefficient of determination (R^2) are reported in graphs.

ACKNOWLEDGMENTS. We thank M. K. Waldor for valuable comments on the manuscript; K. Hayashi for analysis of the circular dichroism spectra; M. Yamamoto and T. Yoshida-Nishimoto for indispensable assistance; S. Uchida, K. Yamashita, A. Goto, M. Kato, N. Suzuki, and S. Hayashi for maintaining the experimental environment; D. Wylie for expert comments on the manuscript; M. Mita and M. Nakane (Shiseido Co. Ltd.) for technical support of the 2D-HPLC; and Collaborative Research Resources, School of Medicine, Keio University for technical support of MALDI-TOF/MS. This study was supported by a Keio University Grant-in-Aid for Encouragement of Young Medical Scientists (to M.S.), the Global Centers of Excellence Program Center for Human Metabolic Systems Biology, Ministry of Education, Culture, Sports, Science, and Technology in Japan (M.S.), the Takeda Science Foundation (J.S.), and Japan Society for the Promotion of Science KAKENHI Grant 21249009 (to S.A.).

1. Hyder F, et al. (2006) Neuronal-glial glucose oxidation and glutamatergic-GABAergic function. *J Cereb Blood Flow Metab* 26(7):865–877.
2. Loaiza A, Porras OH, Barros LF (2003) Glutamate triggers rapid glucose transport stimulation in astrocytes as evidenced by real-time confocal microscopy. *J Neurosci* 23(19):7337–7342.
3. Rothman DL, Behar KL, Hyder F, Shulman RG (2003) In vivo NMR studies of the glutamate neurotransmitter flux and neuroenergetics: Implications for brain function. *Annu Rev Physiol* 65:401–427.
4. Voutsinos-Porche B, et al. (2003) Glial glutamate transporters mediate a functional metabolic crosstalk between neurons and astrocytes in the mouse developing cortex. *Neuron* 37(2):275–286.
5. Cholet N, et al. (2001) Local injection of antisense oligonucleotides targeted to the glial glutamate transporter GLAST decreases the metabolic response to somatosensory activation. *J Cereb Blood Flow Metab* 21(4):404–412.
6. Debernardi R, Magistretti PJ, Pellerin L (1999) Trans-inhibition of glutamate transport prevents excitatory amino acid-induced glycolysis in astrocytes. *Brain Res* 850(1-2):39–46.
7. Gemba T, Oshima T, Ninomiya M (1994) Glutamate efflux via the reversal of the sodium-dependent glutamate transporter caused by glycolytic inhibition in rat cultured astrocytes. *Neuroscience* 63(3):789–795.
8. Ogata T, Nakamura Y, Tsuji K, Shibata T, Kataoka K (1995) A possible mechanism for the hypoxia-hypoglycemia–induced release of excitatory amino acids from cultured hippocampal astrocytes. *Neurochem Res* 20(6):737–743.
9. Choi DW (1990) Possible mechanisms limiting *N*-methyl-D-aspartate receptor overactivation and the therapeutic efficacy of *N*-methyl-D-aspartate antagonists. *Stroke* 21(11, Suppl):III20–III22.
10. Lipton SA (2007) Pathologically activated therapeutics for neuroprotection. *Nat Rev Neurosci* 8(10):803–808.
11. Hardingham GE, Bading H (2010) Synaptic versus extrasynaptic NMDA receptor signalling: Implications for neurodegenerative disorders. *Nat Rev Neurosci* 11(10):682–696.
12. Malinow R (2012) New developments on the role of NMDA receptors in Alzheimer's disease. *Curr Opin Neurobiol* 22(3):559–563.
13. Mothet JP, et al. (2000) D-Serine is an endogenous ligand for the glycine site of the *N*-methyl-D-aspartate receptor. *Proc Natl Acad Sci USA* 97(9):4926–4931.

PNAS PLUS
NEUROSCIENCE
Downloaded at Palestinian Territory, occupied on January 3, 2022
www.manaraa.com

14. De Miranda J, Panizzutti R, Foltyn VN, Wolosker H (2002) Cofactors of serine racemase that physiologically stimulate the synthesis of the *N*-methyl-D-aspartate (NMDA) receptor coagonist D-serine. *Proc Natl Acad Sci USA* 99(22):14542–14547.
15. Neidle A, Dunlop DS (2002) Allosteric regulation of mouse brain serine racemase. *Neurochem Res* 27(12):1719–1724.
16. Kim PM, et al. (2005) Serine racemase: Activation by glutamate neurotransmission via glutamate receptor interacting protein and mediation of neuronal migration. *Proc Natl Acad Sci USA* 102(6):2105–2110.
17. Hikida T, et al. (2008) Modulation of D-serine levels in brains of mice lacking PICK1. *Biol Psychiatry* 63(10):997–1000.
18. Ma TM, et al. (2013) Pathogenic disruption of DISC1-serine racemase binding elicits schizophrenia-like behavior via D-serine depletion. *Mol Psychiatry* 18(5):557–567.
19. Dumin E, et al. (2006) Modulation of D-serine levels via ubiquitin-dependent proteasomal degradation of serine racemase. *J Biol Chem* 281(29):20291–20302.
20. Mustafa AK, et al. (2007) Nitric oxide S-nitrosylates serine racemase, mediating feedback inhibition of D-serine formation. *Proc Natl Acad Sci USA* 104(8):2950–2955.
21. Mustafa AK, et al. (2009) Glutamatergic regulation of serine racemase via reversal of PIP2 inhibition. *Proc Natl Acad Sci USA* 106(8):2921–2926.
22. Pauwels PJ, Opperdoes FR, Trouet A (1985) Effects of antimycin, glucose deprivation, and serum on cultures of neurons, astrocytes, and neuroblastoma cells. *J Neurochem* 44(1):143–148.
23. Wick AN, Drury DR, Nakada HI, Wolfe JB (1957) Localization of the primary metabolic block produced by 2-deoxyglucose. *J Biol Chem* 224(2):963–969.
24. Barban S, Schulze HO (1961) The effects of 2-deoxyglucose on the growth and metabolism of cultured human cells. *J Biol Chem* 236:1887–1890.
25. Xi X, Han J, Zhang JZ (2001) Stimulation of glucose transport by AMP-activated protein kinase via activation of p38 mitogen-activated protein kinase. *J Biol Chem* 276(44):41029–41034.
26. Almeida A, Moncada S, Bolaños JP (2004) Nitric oxide switches on glycolysis through the AMP protein kinase and 6-phosphofructo-2-kinase pathway. *Nat Cell Biol* 6(1): 45–51.
27. Miya K, et al. (2008) Serine racemase is predominantly localized in neurons in mouse brain. *J Comp Neurol* 510(6):641–654.
28. Benneyworth MA, Li Y, Basu AC, Bolshakov VY, Coyle JT (2012) Cell-selective conditional null mutations of serine racemase demonstrate a predominate localization in cortical glutamatergic neurons. *Cell Mol Neurobiol* 32(4):613–624.
29. Ehmsen JT, et al. (2013) D-Serine in glia and neurons derives from 3-phosphoglycerate dehydrogenase. *J Neurosci* 33(30):12464–12469.
30. Yang JH, et al. (2010) Brain-specific Phgdh deletion reveals a pivotal role for L-serine biosynthesis in controlling the level of D-serine, an *N*-methyl-D-aspartate receptor coagonist, in adult brain. *J Biol Chem* 285(53):41380–41390.
31. Yoshida K, et al. (2004) Targeted disruption of the mouse 3-phosphoglycerate dehydrogenase gene causes severe neurodevelopmental defects and results in embryonic lethality. *J Biol Chem* 279(5):3573–3577.
32. Jaeken J, et al. (1996) 3-Phosphoglycerate dehydrogenase deficiency and 3-phosphoserine phosphatase deficiency: Inborn errors of serine biosynthesis. *J Inherit Metab Dis* 19(2):223–226.
33. Panatier A, et al. (2006) Glia-derived D-serine controls NMDA receptor activity and synaptic memory. *Cell* 125(4):775–784.
34. Papouin T, et al. (2012) Synaptic and extrasynaptic NMDA receptors are gated by different endogenous coagonists. *Cell* 150(3):633–646.
35. Basu AC, et al. (2009) Targeted disruption of serine racemase affects glutamatergic neurotransmission and behavior. *Mol Psychiatry* 14(7):719–727.
36. Chaneton B, et al. (2012) Serine is a natural ligand and allosteric activator of pyruvate kinase M2. *Nature* 491(7424):458–462.
37. De Miranda J, Santoro A, Engelender S, Wolosker H (2000) Human serine racemase: Moleular cloning, genomic organization and functional analysis. *Gene* 256(1-2): 183–188.
38. Goto M, et al. (2009) Crystal structure of a homolog of mammalian serine racemase from *Schizosaccharomyces pombe*. *J Biol Chem* 284(38):25944–25952.
39. Wolosker H, Mori H (2012) Serine racemase: An unconventional enzyme for an unconventional transmitter. *Amino Acids* 43(5):1895–1904.
40. Zimmermann H (1994) Signalling via ATP in the nervous system. *Trends Neurosci* 17(10):420–426.
41. Hansson E, Rönnbäck L (2003) Glial neuronal signaling in the central nervous system. *FASEB J* 17(3):341–348.
42. Wilhelm F, Hirrlinger J (2011) The NAD^+/NADH redox state in astrocytes: Independent control of the NAD^+ and NADH content. *J Neurosci Res* 89(12):1956–1964.
43. Kasischke KA, Vishwasrao HD, Fisher PJ, Zipfel WR, Webb WW (2004) Neural activity triggers neuronal oxidative metabolism followed by astrocytic glycolysis. *Science* 305(5680):99–103.
44. Wolosker H, Blackshaw S, Snyder SH (1999) Serine racemase: A glial enzyme synthesizing D-serine to regulate glutamate–*N*-methyl-D-aspartate neurotransmission. *Proc Natl Acad Sci USA* 96(23):13409–13414.
45. Balu DT, Takagi S, Puhl MD, Benneyworth MA, Coyle JT (2014) D-Serine and serine racemase are localized to neurons in the adult mouse and human forebrain. *Cell Mol Neurobiol* 34(3):419–435.
46. O'Mara S (2005) The subiculum: What it does, what it might do, and what neuroanatomy has yet to tell us. *J Anat* 207(3):271–282.
47. Miyoshi Y, et al. (2012) Alteration of intrinsic amounts of D-serine in the mice lacking serine racemase and D-amino acid oxidase. *Amino Acids* 43(5):1919–1931.
48. Miyoshi Y, et al. (2009) Determination of D-serine and D-alanine in the tissues and physiological fluids of mice with various D-amino acid oxidase activities using two-dimensional high-performance liquid chromatography with fluorescence detection. *J Chromatogr B Analyt Technol Biomed Life Sci* 877(24):2506–2512.
49. Suzuki M, et al. (2012) Type 1 diabetes mellitus in mice increases hippocampal D-serine in the acute phase after streptozotocin injection. *Brain Res* 1466:167–176.
50. Miyoshi Y, Oyama T, Itoh Y, Hamase K (2014) Enantioselective two-dimensional high-performance liquid chromatographic determination of amino acids: Analysis and physiological significance of D-amino acids in mammals. *Chromatography* 35(1):49–57.

Downloaded at Palestinian Territory, occupied on January 3, 2022
www.manaraa.com